Meas. Sci. Technol. **16** (2005) 1593–1599 doi:10.1088/0957-0233/16/8/008

A new measurement method for capacitance transducers in a distance compensated telemetric sensor system

Daniele Marioli, Emilio Sardini, Mauro Serpelloni and Andrea Taroni

Department of Electronic Automation, University of Brescia, Via Branze 38, 25123 Brescia (BS), Italy

Received 2 March 2005, in final form 11 May 2005
Published 29 June 2005
Online at stacks.iop.org/MST/16/1593

Abstract
A measurement method for an inductive telemetric system useful for capacitance transducers is described. It is based on a physical model that also considers the leakage and coupled magnetic fluxes and the possible presence of parasitic elements. The model behaviour explains well the measured impedance diagram. Moreover it compensates the change of distance between the read-out and sensing inductors. The method has been experimentally tested showing good agreement with the reference quantities (about 0.6% of the reading value) and compared with a different one. A comparison with a measurement method usually proposed in the literature highlights the distance compensation and the possibility of a more general application. Theoretical explanations, experimental results and discussion are reported.

Keywords: contactless, telemetry, planar inductor, coupled inductors

1. Introduction

In some applications, the measuring environment has characteristics unsuitable for the correct working of the electronics, for example in the industrial field when high temperatures are incompatible with electronics, or it is not accessible, like hermetic boxes or others, for example in the alimentary field when the packages are hermetically closed with modified atmosphere or inside the human body or upon rotating systems. For these cases, it could not be possible to connect the sensitive element to the conditioning electronics by the standard cables. An alternative solution, such as that offered by wireless techniques, does not offer a definitive solution, because they require maintenance due to the periodic substitution of the power supply needed by the active circuits. Telemetric systems can represent valid solutions since they do not require power supply and a wiring linking.

Literature reports some methods and prototypes about telemetric systems and methods. As an example the contactless transmission methodology matched with pressure sensors is quoted: these systems are used in many fields, from industrial control processes [1–3] to biomedical systems [4–6]. Reference [4] is an example where the sensitive element is an inductor–capacitor resonant circuit, made by a capacitive pressure sensor in parallel with an internal planar coil. In the field of industrial application humidity monitoring using electrical capacitance changing could be quoted [2]: the transducer is a passive resonant element made of an inductor and a capacitive humidity sensor.

A telemetric system consists of two planar inductors: one is connected to the sensing element, commonly a capacitance transducer, and the other to the measuring circuit. The first one is a planar, spiral-shaped inductor and can also be integrated together with the sensor, while the second is normally a commonly wired inductance. The two inductors are coupled by a magnetic field, and they are placed at a fixed distance. Some different measurement methods are reported in literature; they are all, anyway, based on the impedance measurement to identify a particular frequency, a resonance in some cases or a minimum phase point, related to the quantity under measurement.

In the paper a new measurement method is proposed: it can be applied to describe the behaviour of more general telemetric systems such as those constituted by only planar

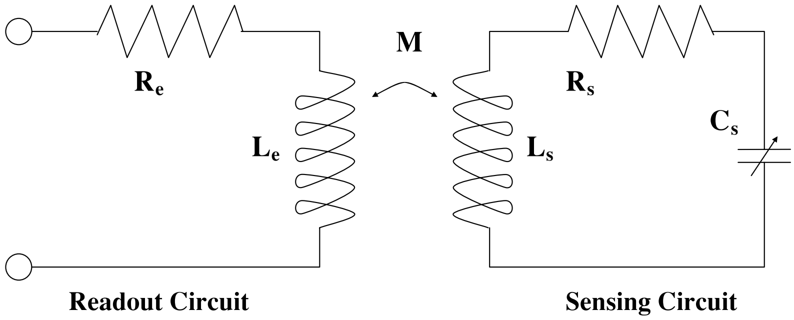

Figure 1. A model commonly used to analyse telemetric systems.

inductors. It also compensates the change of distance between the two inductors. The telemetric system is modelled keeping in consideration the effects induced by the changes of leakage flux and also the presence of the parasitic capacitances. In this way the diagram of the impedance experimentally measured on the terminals of a real measuring inductor, where two resonance and one anti-resonance frequencies are present, is in agreement with the model behaviour.

In the following sections the method proposed is theoretically described and experimentally tested; each element of the model used to derive the method is identified with the corresponding physical principle; an approximation on the coupling capacitance is introduced and justified. The mathematical relation between the impedance measured and the transducer capacitance is reported. After that a telemetric system has been made and experimentally tested on an experimental apparatus, showing good agreement with the reference quantities.

In order to validate the proposal, a comparison with a measurement method usually proposed in the literature (called in the following the min-phase method) has been made by both discussing the theoretical differences and analysing the experimental results of each method. For this reason also the min-phase method is synthetically introduced.

2. Model and measurement method

2.1. The min-phase method

In the previous papers [1–6], the inductive telemetric systems consist of a planar inductance, in the sensing circuit, and a coil inductance, in the read-out circuit, with a diameter much larger than that of the planar one. Figure 1 reports the equivalent circuit: the planar inductance is modelled with an inductor (L_s), a series parasitic resistance (R_s) and a variable capacitor (C_s) representing the capacitance sensor. The read-out circuit is modelled with an inductor (L_e) and a series parasitic resistance (R_e). When the two circuits are closed, there is a mutual inductance coupling (M) between the inductor L_s and the inductor L_e. The read-out circuit measures the impedance and the frequency at which the phase, in a short frequency interval, is at its minimum value; this frequency corresponds to

$$f_0 = \frac{1}{2\pi\sqrt{L_s C_s}}. \tag{1}$$

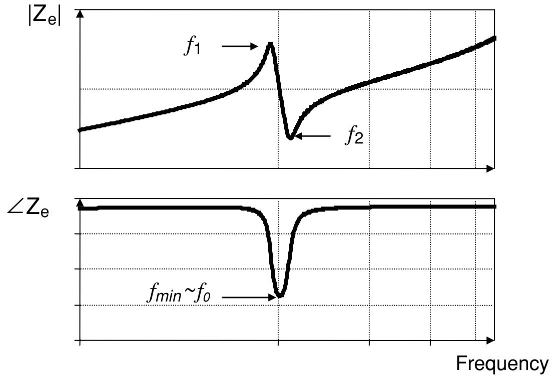

Figure 2. Qualitative trend of the impedance Z_e for a short interval around f_0.

In fact the total impedance, as seen from the terminals of the read-out circuit, is given by [7]

$$Z_e(\omega) = R_e + j\omega L_e + \frac{\omega^2 M^2}{Z_s(\omega)}, \tag{2}$$

with

$$Z_s(\omega) = R_s + j\omega L_s - j\frac{1}{\omega C_s}. \tag{3}$$

At the resonance frequency f_0 ($f_0 = \omega_0/2\pi$), equation (2) becomes

$$Z_e(\omega_0) = R_e + j\omega_0 L_e + \frac{\omega_0^2 M^2}{R_s}, \tag{4}$$

and its phase, for a short frequency interval close to f_0, reaches the minimum value at f_{min}, as shown in figure 2. Paper [1] explains that the frequency at the phase minimum (f_{min}) is related to f_0 from expression (5), which corresponds to the Taylor expansion of f_{min} in k (coupling coefficient) and Q^{-1} (quality factor of the sensing circuit).

$$f_{min} = f_0\left(1 + \frac{k^2}{4} + \frac{1}{8Q^2}\right). \tag{5}$$

With $k = M/\sqrt{L_e L_s}$, the expression denotes that a distance change affects the coupling factor and consequently f_{min}.

However, it is important to note that the method works correctly if the self-resonance frequency of the inductors is much higher than f_0 and the distance between the two inductors is fixed.

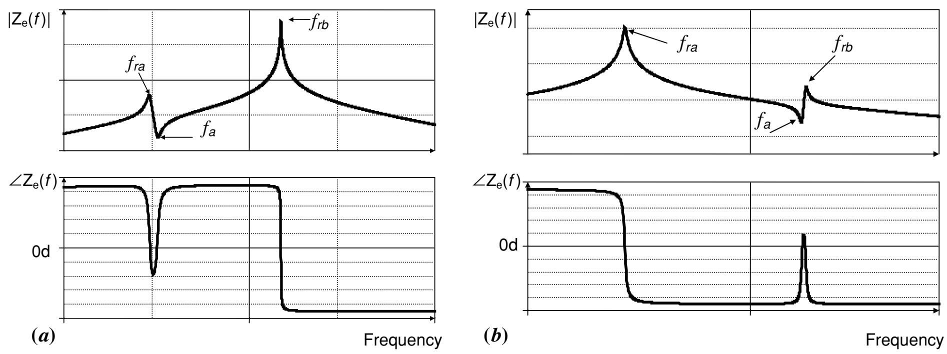

Figure 3. Qualitative impedance diagrams as seen from the read-out circuit. The self-resonance of the read-out inductor is close to f_{rb} (*a*) or f_{ra} (*b*).

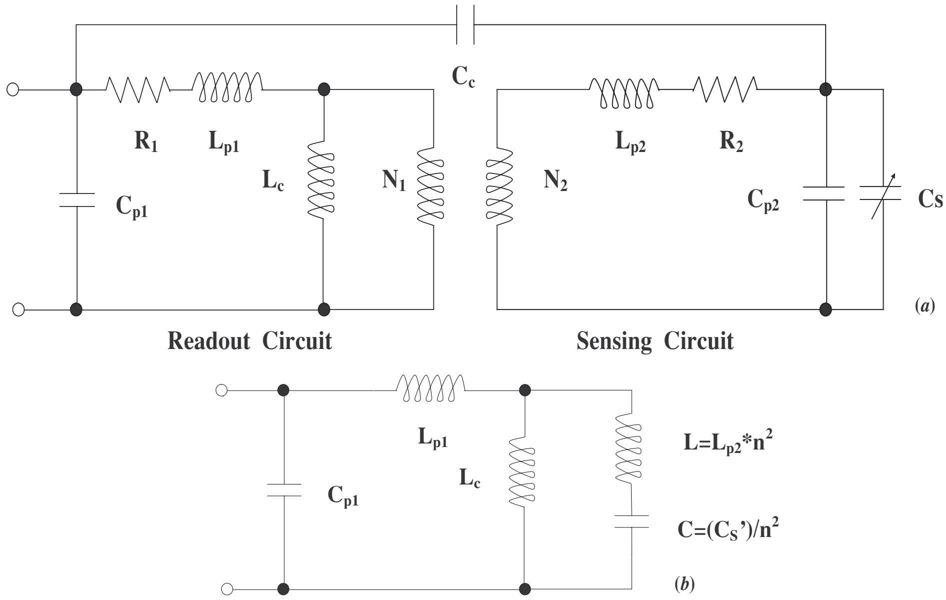

Figure 4. The proposed model: (*a*) the complex model; (*b*) a simplified version that neglects the coupling capacitance between the two inductors.

2.2. The method proposed

The previous model neglects the parasitic capacitances and, also, the leakage flux is not directly considered, even if coefficient M keeps in consideration the coupled magnetic flux. Although in many applications the model describes sufficiently the behaviour of two coupled inductors, experimental measurements give results whose interpretation requires a more detailed model. Figures 3(*a*) and (*b*) show some typical diagrams of experimental impedance measurements (module and phase) obtained from the read-out circuit. In both cases there are three noticeable frequencies f_{ra}, f_{rb} and f_{a}: in (*a*) f_{ra} and f_{a} correspond to f_1 and f_2 (see figure 2) while f_{rb} is mainly due to the self-resonance of the read-out inductor; in (*b*) f_{ra} is mainly due to the self-resonance of the read-out circuit while f_{a} and f_{rb} depend on the transducer capacitance. The min-phase method can be applied only in case (*a*).

The measured impedance diagrams are better explained applying the physical model shown in figure 4(*a*). The parameters have the following meaning: R_1, equivalent resistance of read-out inductance; R_2, equivalent resistance of sensing circuit inductance; C_{p1}, inter-winding capacitance of read-out spiral; C_{p2}, inter-winding capacitance of sensing circuit spiral; C_{c}, coupling capacitance between sensing circuit and read-out; C_{s}, sensing capacitance; L_{c}, inductance representing the coupling flux; L_{p1}, read-out leakage inductance; L_{p2}, sensing circuit leakage inductance. N_1 and N_2 are the turns of the inductor: quantifying a turn for a planar spiral- or square-shaped inductor is not an easy task but these parameters will disappear from the final relationship. While for physical explanation the parasitic and transducer capacitances have been separated into two elements in the model, for practical reasons they will join into C_{s}' equal to the sum of C_{s} and C_{p2}.

The coupling capacitance C_{c} considers the effect of the electric field coupled between the conducting tracks of the two inductors; its value is generally low even for close distance and can be further minimized by increasing the distance between both the two inductors and each inductor track. For this reason, in the following C_{c} is neglected and the model of figure 4(*a*) can be simplified into that shown in figure 4(*b*) where the elements of the sensing circuit are brought to the read-out circuit. L and C are L_{p2} and C_{s}' as seen from the primary of the ideal transformer and the parameter n is the ratio between N_1 and N_2.

If the simplified model is considered, the impedance at the terminal is

$$Z_e(s) = \{s^3(L_cLC + L_{p1}C(L_c + L)) + s(L_c + L_{p1})\}/ \{s^4C_{p1}(L_cLC + L_{p1}C(L_c + L)) + s^2(C_{p1}(L_c + L_{p1}) + C(L_c + L)) + 1\}. \quad (6)$$

The impedance reported in (6) has a frequency diagram that justifies the resonance and anti-resonance frequencies shown in the measured impedance diagram of figure 3. The first (f_{ra}) and second resonance frequencies (f_{rb}) have complicated expressions and they are reported in the appendix. They are both influenced by C_{p1} and C'_s. The anti-resonance frequency (f_a) is influenced only by C'_s and it is more sensitive to C'_s than the other two frequencies. The expression for f_a is

$$f_a = \frac{1}{2\pi\sqrt{C\left(L + \frac{L_cL_{p1}}{L_{p1}+L_c}\right)}}. \quad (7)$$

Because f_a depends only on the transducer capacitance, while f_{ra} and f_{rb} depend also on C_{p1}, it seems more useful to measure f_a. Anyway, even if the transducer capacitance is kept constant, but the distance between the read-out and sensing inductances changes, the two resonance and single anti-resonance frequencies change. In fact, when the distance changes, the coupled and leakage fluxes change too. For f_a this effect is clearly visible by analysing the terms in parenthesis of equation (7).

It is possible to derive a parameter F that depends only on distance. It expression is

$$F = ((2\pi f_{ra})^2 + (2\pi f_{rb})^2) - (2\pi f_a)^2 = \frac{1}{C_{p1}\left(L_{p1} + \frac{L_cL}{L_c+L}\right)}. \quad (8)$$

If C_{p1} is fixed, F depends only on coupled and leakage fluxes: these values are related only to the distance and not to the transducer capacitance. Moreover, the parameter F can be calculated by the measurement of f_{ra}, f_{rb} and f_a.

Rearranging the previous equations, a straightforward expression of the sensor capacitance (C'_s), also compensated in distance, can be obtained:

$$C'_s = \frac{L_1C_{p1}}{L_2}\frac{F}{(2\pi f_a)^2}. \quad (9)$$

C'_s is obtained as a product of a constant term and a second one calculated from the three measured frequencies f_{ra}, f_{rb} and f_a. The constant term can be automatically obtained from a calibration operation or can be calculated measuring the equivalent circuit parameters of each single planar inductor: L_1 and L_2 are the self-inductances of the read-out and sensing inductances, while C_{p1} is the parasitic capacitance (or any other added capacitance) of the read-out circuit.

Equation (9) has been derived with no restricting hypothesis and maintains its significance also when the self-resonance of the read-out circuit is lower than f_0 (case (*b*) of figure 3). It obviously maintains its significance also for case (*a*) of figure 3.

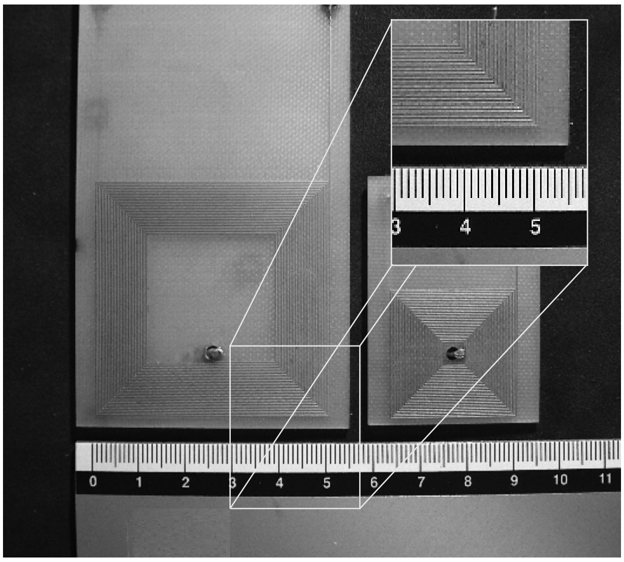

Figure 5. Planar inductors realized. The scale unit is centimetre.

3. Experimental apparatus and its characterization

To experimentally verify the method proposed, a telemetric system and its support system have been made. Figure 5 shows a photo of the telemetric system consisting of two planar inductors whose shape is square. The read-out planar inductor (on the left) consists of 27 turns of square tracks and has an external width of 50 mm. Each trace is 0.2 mm wide and the space between them is 0.22 mm. The sensing inductor is yet square shaped with the same number of turns and space between lines; its external width is 27 mm. The external width of the sensing inductor is equal to the width of the inner hole of the read-out circuit. Since the two inductances are placed facing one another with their central axes coincident, the conductive tracks are oblique and the coupling capacitance is reduced.

An L-shaped support fixes the two inductors; these inductors are placed horizontally, facing one another with the two central axes coincident. The support is made of wood to reduce possible parasitic effects induced by the presence of metallic elements close to the measurement environment. The inductor clamp is plastic and the handling system is an aluminium micrometer screw. Figure 6 reports a photo of the supporting system. It is possible to note the presence of two micrometer screws: the vertical one regulates the distance between the two inductors from 0 to 25 mm, while the horizontal one is used for alignment purposes.

The self-inductances and parasitic capacitances have been measured by an HP 4194A impedance analyser modelling each planar inductor like a classical circuit consisting of a series of inductance (L_{ser}) and resistor (R_{ser}) both in parallel to a capacitance (C_{par}). Values measured are reported in table 1. The self-resonances of the two inductors are 13 and 28 MHz approximately for the read-out and sensing circuits, respectively.

Since previous considerations lead to neglecting the coupling capacitance, to verify the correctness of this hypothesis its value has been measured and compared with those of the other capacitances. Figure 7 shows the coupling

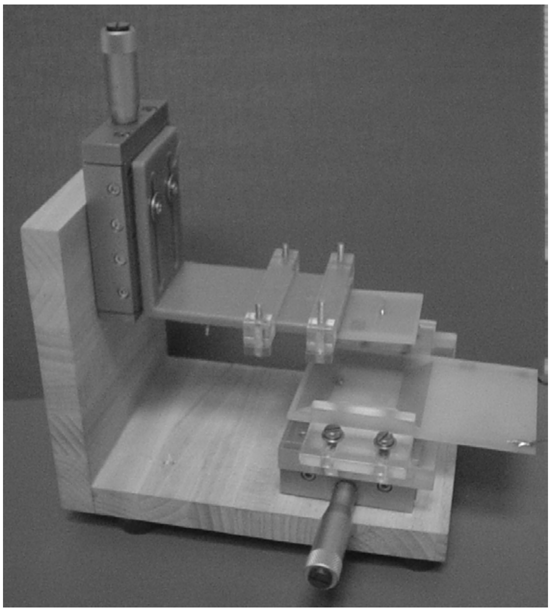

Figure 6. Experimental apparatus.

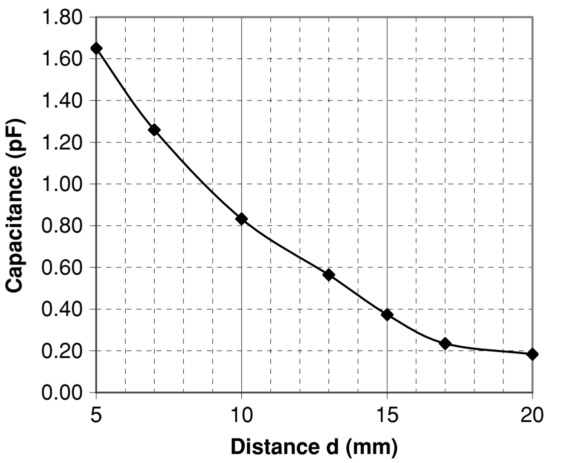

Figure 7. Coupling capacitance as a function of the distance.

Table 1. Values of equivalent circuit parameters for the planar inductors not coupled.

Inductor	L_{ser} (H)	R_{ser} (Ω)	C_{par} (F)
Readout	46.69×10^{-6}	26.05	3.15×10^{-12}
Sensing	12.10×10^{-6}	20.62	2.6×10^{-12}

capacitance as a function of the distance. For all the distance interval, the measured value is much less than those of the parasitic capacitances of each inductor.

4. Experimental results

A set of experimental tests on the telemetric system has been carried out varying the sensing capacitance and also the distance between the two planar inductors. To simulate a transducer capacitance, six different values over a wide range of commercial capacitors have been chosen. Their values have been measured by the HP 4194A impedance analyser and in

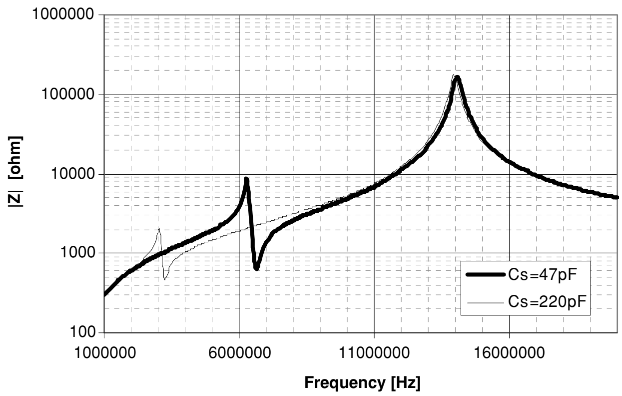

Figure 8. Impedance module measured by HP4194A with C_s = 47 pF @ 5 mm and C_s = 220 pF @ 5 mm.

Table 2. Reference capacitance values.

Nominal (pF)	Measured C_s (pF)	Reference C'_s (pF)
47	48.700	51.300
68	67.000	69.600
100	99.490	102.090
150	144.720	147.320
180	170.255	172.855
220	216.195	218.795

table 2 their nominal and measured values are reported in the first two columns. Since the parasitic capacitances of the sensing inductor are parallel to the capacitor, its value has been added to the previous measured values and the results, shown in the third column, are the reference ones.

After mounting the experimental apparatus and placing the reference capacitance on the two sensing inductor, the impedance on the read-out has been measured by the HP 4194A impedance analyser and the graphs obtained are reported in figure 8: the two resonance and the anti-resonance frequencies are clearly visible. The second resonance is close to the self-resonance of the read-out circuit, that is the condition required by the correct application of the min-phase method. In this case, it is possible to measure the capacitance according to both methods for comparison purposes. Consequently for each impedance diagram, the frequencies f_{ra}, f_{rb}, f_a and f_o have been measured.

While keeping constant all the other parameters, the distance between the two coupled planar inductors has been changed from 5 mm to 20 mm by a micrometric screw.

While decreasing the lower value of this interval increases the coupling capacitance, the upper limit depends on measurement electronics resolution. In fact the coupled flux decreases. In fact the coupled flux decreases at greater distance: both the peak and the valley of f_{ra} and f_a come close to each other and overlap.

Figure 9 reports the F values as a function of distance, and for different reference capacitances, these values have been calculated from equation (8) and using the measured f_{ra}, f_{rb} and f_a frequencies. Analysing the graph, F depends mainly on distance, and is almost independent of different values of C'_s, in agreement with the theoretical analysis. The same F values have been used to calculate, according to equation (9), the C'_s

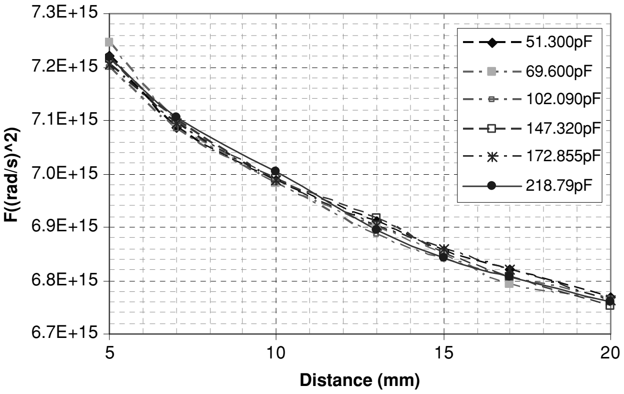

Figure 9. Parameter F as a function of the distance.

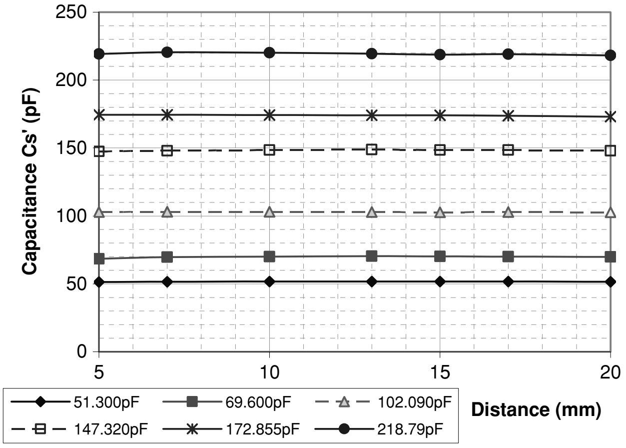

Figure 10. Capacitive values determined with the proposed method.

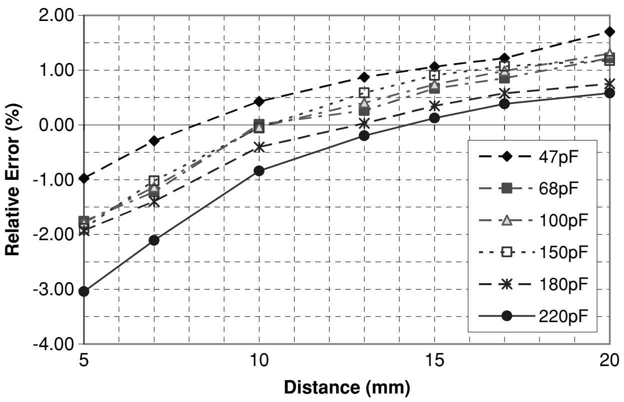

Figure 11. Relative error calculated with the min-phase method.

values and figure 10 reports the result obtained, demonstrating that these measured values are almost insensitive to distance variation.

The capacitance values according to the min-phase method have been calculated and their relative errors with respect to the reference ones are reported in figure 11. It is noticed that relative error increases with the distance: this behaviour depends on the shift of f_0 due to the change of the leakage and coupling fluxes. The span for each capacitance value over the distance interval is about 2.5–3.5 points.

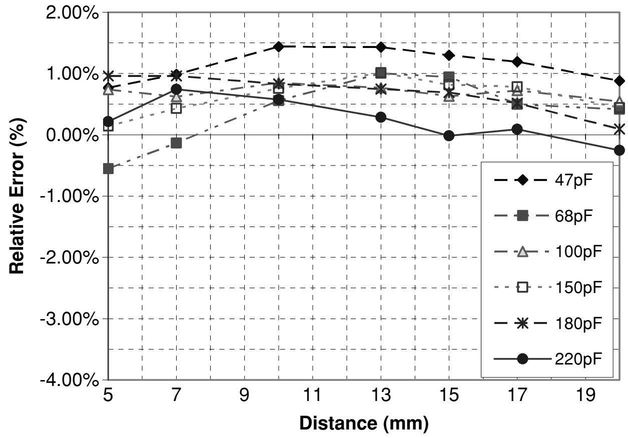

Figure 12. Relative error calculated with the method proposed.

Figure 12 reports the relative error between the reference values and those obtained with the method proposed. As can be seen the results seem to show no dependence on the distance and the average span is reduced: in fact for each capacitance over the distance interval, its span is from 0.6 to 1.5 points. Moreover, the calculated values are almost always more positive than the reference ones. Probably a more accurate value of the constant term (L_1 and L_2 self-inductances and C_{p1} parasitic capacitance) can reduce the absolute error values. This reduction can also be obtained by performing a calibration operation. Moreover, it seems correct to have neglected the contribution from the coupling capacitance; in the distance interval, its value constantly decreases by an order of magnitude, while the trend of the interpolation function is ambiguous and with a low span.

5. Conclusion

A new measurement method for a telemetric system based on capacitance transducer has been proposed. It uses a more complete model that considers the presence of the parasitic effects and of the leakage and coupled fluxes. For this reason the model can be applied, with no restricting hypothesis, to many different telemetric systems including also those consisting of two planar inductors and having transducer capacitance of the same order as the parasitic capacitance of the inductors. The model introduced matches well the impedance diagrams as measured from the read-out circuit, and the approximation introduced is justified by the lack of dependence of the experimental data on the coupling capacitance.

The measurement method compensates the change of distance between the two inductors. The method has been tested, measuring reference capacitance cross calibrated with an accurate impedance analyser. It has also been compared with a different measurement method, commonly used for telemetric applications reported in the literature, showing the possibility of obtaining reduced relative errors of about 0.6% points of the reading.

The distance interval has been set between 5 and 20 mm, being the low and high values depending on the increase of the coupling capacitance and decrease of the coupled flux, respectively. Because our aim was to investigate a measurement method with the distance compensation, we do not extend the distance interval over the limit where the inaccuracies in the measurement should be attributed to other factors. Moreover, we are confident that the measurement method proposed can be applied to different inductive telemetric systems where the interval distance can be further extended.

Appendix

In this appendix some simple steps to determinate the mathematical expression used in (9) are reported.

Expression (6) is reported as follows:

$$Z_e(s) = \{s^3(L_cLC + L_{p1}C(L_c + L)) + s(L_c + L_{p1})\}/ \{s^4C_{p1}(L_cLC + L_{p1}C(L_c + L)) + s^2(C_{p1}(L_c + L_{p1}) + C(L_c + L)) + 1\}. \tag{A1}$$

The numerator and the denominator are put equal to zero and resolved. The numerator gives an expression (A2) to determine the resonance frequencies f_{ra} and f_{rb}:

$$(2\pi f_{ra,b})^2 = \frac{1}{2C\left(L + \frac{L_{p1}L_c}{L_{p1}+L_c}\right)} + \frac{1}{2C_{p1}\left(L_{p1} + \frac{LL_c}{L+L_c}\right)} \pm \left\{ \frac{1}{4C^2\left(L + \frac{L_{p1}L_c}{L_{p1}+L_c}\right)^2} - \frac{1}{4C_{p1}^2\left(L_{p1} + \frac{LL_c}{L+L_c}\right)^2} - \frac{L_c^2 - L_{p1}L_c - LL_{p1} - LL_c}{2CC_{p1}(LL_{p1} + LL_c + L_{p1}L_c)^2} \right\}^{1/2}. \tag{A2}$$

Instead the denominator gives

$$(2\pi f_a)^2 = \frac{1}{C\left(L + \frac{L_cL_{p1}}{L_c+L_{p1}}\right)} \tag{A3}$$

To determine the expression of the parameter F, it is observed that the sum of the square of the two resonance pulsations is quite simple and contains the anti-resonance pulsation.

$$(2\pi f_{ra})^2 + (2\pi f_{rb})^2 = \frac{1}{C\left(L + \frac{L_{p1}L_c}{L_{p1}+L_c}\right)} + \frac{1}{C_{p1}\left(L_{p1} + \frac{LL_c}{L+L_c}\right)}. \tag{A4}$$

So the parameter F can thus be determined as

$$F = ((2\pi f_{ra})^2 + (2\pi f r_{rb})^2) - (2\pi f_a)^2 = \frac{1}{C_{p1}\left(L_{p1} + \frac{L_cL}{L_c+L}\right)}. \tag{A5}$$

It is recalled that the expressions for the sensing circuit inductor and read-out inductor are as follows:

$$L_1 = L_{p1} + L_c \tag{A6}$$

$$L_2 = L_{p2} + \frac{L_c}{n^2}. \tag{A7}$$

Below expression (9) to calculate the sensing capacitance obtained with the previous expressions is reported:

$$C_s' = \frac{L_1C_{p1}}{L_2}\frac{F}{(2\pi f_a)^2}. \tag{A8}$$

References

[1] Fonseca M A, English J M, von Arx M and Allen M G 2002 Wireless micromachined ceramic pressure sensor for high temperature applications *J. Microelectromech. Syst.* **11** 337–43

[2] Harpster T, Stark B and Najafi K 2002 A passive wireless integrated humidity sensor *Sensors Actuators* A **95** 100–7

[3] Todoroki A, Miyatani S and Shimamura Y 2003 Wireless strain monitoring using electrical capacitance change of tire: Part II. Passive *Smart Mater. Struct.* **12** 410–6

[4] Akar O, Akin T and Najafi K 2001 A wireless batch sealed absolute capacitive pressure sensor *Sensors Actuators* A **95** 29–38

[5] Hamici Z, Itti R and Champier J 1996 A high-efficiency power and data transmission system for biomedical implanted electronic device *Meas. Sci. Technol.* **7** 192–201

[6] Schnakenberg U, Walter P and vom Bogel G 2000 *Initial investigations on systems for measuring intraocular pressure* Institute for Materials in Electrical Engineering, Aachen, Germany

[7] Terman F E 1943 *Radio Engineering's Handbook* (New York: McGraw-Hill)